

A CFD/CSD Model for Transonic Flutter

Tong-qing Guo, Zhi-liang Lu¹

Abstract: In this paper, a rapid deforming technique is developed to generate dynamic, three-dimensional, multi-block, mesh. The second-order Runge-Kutta time-marching method is used to solve the structural equations of motion. A dual-time method and finite volume discretization are applied for the unsteady Euler/Navier-Stokes equations to calculate the aerodynamic forces, in which the physical time step is synchronous with the structural equations of motion. The Spalart-Allmaras turbulence model is adopted for a turbulent flow. Due to mass dissimilarity, existing in flutter calculations for a compressible flow, methods of variable mass and variable stiffness are developed to calculate the dynamic pressure of flutter at the point of mass similarity, and the flutter characteristics are then obtained in accordance with similarity rule. For completeness, the calculated transonic flutter characteristic results are presented and discussed for a double-wing and an aircraft model.

keyword: Flutter, Transonic flow, Unsteady flow, Euler/Navier-Stokes equations, Structural equations

1 Introduction

In recent years, computational fluid dynamics (CFD) has been developed very fast. Some new developments have been made for the simulation of incompressible and turbulent flows [Shu, Ding and Yeo (2004); Wang, Zhang, Chan and Wang (2004)]. In flutter computations for aircraft, the calculation is usually done in the frequency domain [De (1994)], where the unsteady aerodynamic forces are all calculated by the doublet lattice method based on the linear theory, and the computational method for transonic flutter is usually a rough deducting method, namely a deduction of an appropriate empirical percent from the transonic results. The way is difficult to evaluate the flutter characteristics accurately because the flutter shape differs considerably from one kind of vehicle to

another. Hence, it is necessary to develop a computational method based on the non-linear aerodynamic equations for transonic flutter.

The transonic unsteady aerodynamic forces can be calculated by solving small perturbation, full-potential [Lu (2001)] or Euler/Navier-Stokes equations, and then the calculated aerodynamic forces can be directly applied to flutter computations in the frequency domain. Coupled with the structural equations of motion, the happening of flutter can be judged by calculating the generalized coordinate time response in the time domain.

In the present paper, the second-order Runge-Kutta time-marching method is used to solve the structural equations of motion. The finite-volume spatial discretisation [P'ascoa, Mendes, Gato and Elder (2004); Jameson, Schmidt and Turkel, (1981); Jameson, Schmidt and Whitfield (1981)] is applied to the unsteady Euler/Navier-Stokes equations, and then the time-accurate aerodynamic forces are calculated by a dual-time method [Gationde (1995)], in which the physical time step is synchronous with the structural equations of motion. In a physical time step, the aerodynamic equations are marched to a steady state in pseudo time using a hybrid multistage Runge-Kutta method. For a turbulent flow, the Spalart-Allmaras [Spalart and Allmaras (1992)] one-equation turbulence model is adopted.

Similar to a transonic flutter experiment, mass dissimilarity would sometimes exist in the calculated dynamic pressure for a compressible flow at a given freestream Mach number, that is, the fluid density inversely evaluated from the calculated flutter dynamic pressure may be much larger than that in the flight condition. In engineering, the density must be matched to obey the similarity rule in order to confirm a practicable margin of the dynamic pressure of flutter. At present work, methods of variable mass and variable stiffness are developed to calculate the dynamic pressure of flutter at the point of mass similarity, and the practicable transonic flutter characteristics are then obtained by analyzing the trend

¹ Department of Aerodynamics, Nanjing University of Aeronautics and Astronautics, China 210016, luzl@nuaa.edu.cn

of the dynamic pressure of flutter varying with the multiples of variable mass or variable stiffness. For completeness, the transonic flutter characteristic results calculated using the method are shown for a double-wing and an aircraft model.

2 Multi-block Grid Generation

The hybrid algebraic/elliptic differential equation method is applied to generate multi-block static grids for an aircraft configuration. For unsteady computations with moving walls, the dynamic grids are adopted, whose outer boundaries (far-field or block boundary) are fixed and the inner ones (solid wall) move synchronously with the motion or deformation of the solid walls. Since the generation of grid is required for every time step and it is very time-consuming, an approximately simplified method is developed to generate three-dimensional multi-block dynamic grids. At first, the instantaneous boundary grids of each block are generated, and then a rapid deforming technique [Lu (2001)] is used to evaluate the dynamic coordinates for the inner grid nodes of each block. The coordinates of the dynamic grid node (denoted by the subscript u) is given by

$$x_u = x_r - (x_r - x_s) \cdot g \quad (1)$$

where the subscript s denotes the coordinates of the initial static grid node, r the instantaneous coordinates when the static grid node moves synchronously with the solid walls, and g is a function of the grid node given by

$$g = \max \left(\left(\frac{i - i_b}{i_f - i_b} \right)^2, \left(\frac{j - j_b}{j_f - j_b} \right)^2, \left(\frac{k - k_b}{k_f - k_b} \right)^2 \right) \quad (2)$$

Here the subscript b denotes inner boundary point, f stands for the outer boundary point.

3 Structural Equations of motion

The longitudinal oscillating deformation of the wall surface points of an aircraft is approximately expressed as

$$Z(x, y, t) = \sum_{i=1}^n h_i(x, y) q_i(t) \quad (3)$$

and the structural equations of motion are written as

$$[M] \{q_{tt}\} + [G] \{q_t\} + [K] \{q\} = \{A\} \quad (4)$$

where n is the number of the structural mode considered, h the structural mode data of each mode, q the generalized coordinate, M , G and K are the generalized mass, the damping and the stiffness, respectively. Here, $G = 0$, $K_{ii} = \omega_i^2 M_{ii}$, $\omega_i = 2\pi f_i$. The generalized aerodynamic force is given by

$$A_i = \frac{1}{2} \rho V^2 \iint \Delta C_p(x, y, t) h_i(x, y) ds \quad (5)$$

After the instantaneous generalized aerodynamic A is solved from the aerodynamic equations, a state variable $\{E\}$ is introduced to the structural equations of motion, which is defined as

$$\begin{aligned} \{E\} &= [\{q\}^T, \{q_t\}^T]^T \\ &= [q_1, q_2, q_3, \dots, q_n, q_{t1}, q_{t2}, q_{t3}, \dots, q_{tn}]^T \end{aligned} \quad (6)$$

Then equation (4) becomes

$$\begin{aligned} \{E_t\} &= \begin{bmatrix} [0] & [I] \\ -[M]^{-1}[K] & -[M]^{-1}[G] \end{bmatrix}^T \{E\} \\ &+ \begin{bmatrix} [0] \\ [M]^{-1} \end{bmatrix} \{A\} \end{aligned} \quad (7)$$

where $[0]$ represents the zero matrix, $[I]$ the identity matrix.

Equation (7) are solved by the second-order five-stage Runge-Kutta time-marching method.

4 Unsteady Euler/Navier-Stokes Equations On a Moving Mesh

4.1 Governing Equations

In the Cartesian coordinate system, the differential form of the unsteady Euler/Navier-Stokes equations on a moving mesh can be written in terms of non-dimensional variables and in coordinate invariant formulation as

$$\frac{\partial \vec{U}}{\partial t} + \frac{\partial \vec{F}_i}{\partial x_i} = \frac{\partial \vec{G}_i}{\partial x_i} \quad (8)$$

where \vec{U} , \vec{F}_i and \vec{G}_i are respectively the unknown vector, the convective flux vector and the viscous flux vector (equals

to zero for the Euler equations), and they are given by

$$\begin{aligned} \vec{U} &= \begin{bmatrix} \rho \\ \rho u_1 \\ \rho u_2 \\ \rho u_3 \\ \rho E \end{bmatrix} \\ \vec{F}_i &= \begin{bmatrix} \rho U_i \\ \rho u_1 U_i + p \delta_{1i} \\ \rho u_2 U_i + p \delta_{2i} \\ \rho u_3 U_i + p \delta_{3i} \\ (\rho E + p) U_i + (x_i)_t p \end{bmatrix} \\ \vec{G}_i &= \begin{bmatrix} 0 \\ \sigma_{1i} \\ \sigma_{2i} \\ \sigma_{3i} \\ u_m \sigma_{im} + k \cdot \partial T / \partial x_i \end{bmatrix} \end{aligned} \quad (9)$$

In the above, δ_{ij} is the Kronecker symbol, ρ is the fluid density, u_i are the Cartesian components of the fluid velocity, E the total energy and p is the pressure which is obtained from

$$p = (\gamma - 1)[\rho E - \rho(u_i^2)/2] \quad (10)$$

U_i are the components of the contravariant velocity defined by

$$U_i = u_i - (x_i)_t \quad (11)$$

where $(x_i)_t$ are the Cartesian components of the grid speed. The components of the viscous stress tensor σ_{ij} are defined as

$$\sigma_{ij} = 2\mu S_{ij} - \frac{2}{3}\mu \left(\frac{\partial v_k}{\partial x_k} \right) \delta_{ij} \quad (12)$$

where the components of the strain-rate tensor are given by

$$S_{ij} = \frac{1}{2} \left(\frac{\partial v_i}{\partial v_j} + \frac{\partial v_j}{\partial v_i} \right) \quad (13)$$

During the process of coupling the Euler/Navier-Stokes equations with the structural equations of motion, much attention should be paid to the dimension-matching problem of the length and the area when a non-dimensional aerodynamic coefficient is transformed into a dimensional one. The same is applied to the time transformation.

4.2 Dual-Time Marching

The Euler/Navier-Stokes equations on a moving mesh are solved using a cell-centered finite-volume method [Jameson, Schmidt and Turkel (1981); Jameson, Schmidt and Whitfield (1981)], in which the central scheme with JST artificial dissipation [Jameson, Schmidt and Turkel (1981)] is applied. After the finite-volume spatial discretisation is applied to equation (8), the system of equations takes the form

$$\frac{d}{dt}(H_{ijk} \vec{W}_{ijk}) + \vec{R}_{ijk} = 0 \quad (14)$$

where \vec{W} , \vec{H} and \vec{R} are dependent variable, volume and residual respectively, the indices (ijk) reference the control volume. Following the work of Jameson [Jameson (1991)], an implicit algorithm is applied to equation (14) at time level $(n + 1)$,

$$\frac{d}{dt}(H_{ijk}^{n+1} \vec{W}_{ijk}^{n+1}) + R(\vec{W}_{ijk}^{n+1}) = 0 \quad (15)$$

Then a backward second-order finite difference scheme is used to discretize d/dt . As a result, equation (15) becomes

$$\begin{aligned} & \frac{3H_{ijk}^{n+1} \vec{W}_{ijk}^{n+1} - 4H_{ijk}^n \vec{W}_{ijk}^n + H_{ijk}^{n-1} \vec{W}_{ijk}^{n-1}}{2\Delta t} + \vec{R}(\vec{W}_{ijk}^{n+1}) \\ & = \vec{R}^*(\vec{W}_{ijk}^{n+1}) = 0 \end{aligned} \quad (16)$$

Finally, a derivative with respect to a pseudo time, τ , is added to equation (16) to give

$$H_{ijk}^{n+1} \frac{d\vec{W}_{ijk}^{n+1}}{d\tau} + R^*(\vec{W}_{ijk}^{n+1}) = 0 \quad (17)$$

The solution of equation (17) is obtained by marching to a steady state in pseudo time using a hybrid explicit five-stage Runge-Kutta method [Martinelli and Jameson (1990)]. This solution has a feature of

$$\frac{d\vec{W}_{ijk}^{n+1}}{d\tau} = 0 \quad (18)$$

which means that it satisfies $R^*(\vec{W}_{ijk}^{n+1}) = 0$ and hence it is also the solution of equation (15) at time level $(n + 1)\Delta t$.

4.3 Geometric Conservation Law

The geometric conservation law (GCL) [Thomas and Lombard (1979)] must be satisfied in order to avoid errors induced by deformation of control volumes. The integral form of the GCL reads

$$\frac{\partial}{\partial t} \int_{\Omega} d\Omega - \int_{\partial\Omega} \vec{V}_t \cdot \vec{n} dS = 0 \quad (19)$$

where \vec{V}_t , \vec{n} are respectively the velocity vector of the face of the control volume $d\Omega$, the outward facing unit normal vector of the surface $\partial\Omega$. In order to obtain a self-consistent method, the GCL in equation (19) is temporally discretised using the same scheme as applied to the physical conservation laws.

5 Spalart-Allmaras Turbulence Model

For a turbulent flow, the viscosity coefficient and the thermal conductivity coefficient are respectively replaced by

$$\mu = \mu_l + \mu_t, \quad k = k_l + k_t = c_p(\mu_l/Pr_l + \mu_t/Pr_t) \quad (20)$$

The Spalart-Allmaras [Spalart and Allmaras (1992)] one-equation turbulence model employs transport equation for an eddy-viscosity variable $\tilde{\nu}$. It is developed from empiricism, dimensional analysis and Galilean invariance selected dependence on the molecular viscosity. It is calibrated using the experimental results for 2-D mixing layers, wakes, and flat-plate boundary layer, and it also provides accurate predictions of turbulent flows with adverse pressure gradients. The model includes a wall destruction term that reduces the turbulent viscosity in the laminar sublayer. The model takes the form

$$\frac{D\tilde{\nu}}{Dt} = C_{b1}\tilde{S}\tilde{\nu} + \frac{1}{\sigma}[\nabla \cdot ((\mathbf{v} + \tilde{\nu})\nabla\mathbf{v}) + C_{b2}(\nabla\tilde{\nu})^2] - C_{w1}f_w\left(\frac{\tilde{\nu}}{d}\right)^2 \quad (21)$$

The turbulent kinematic viscosity is obtained from

$$\nu_t = \frac{\mu_t}{\rho} = \tilde{\nu}f_{v1}, \quad f_{v1} = \frac{\chi^3}{\chi^3 + C_{v1}^3}, \quad \chi = \frac{\tilde{\nu}}{\nu} \quad (22)$$

Let S denote the magnitude of the vorticity. The modified vorticity is

$$\tilde{S} = S + \left(\frac{\tilde{\nu}}{\kappa^2 d^2}\right) f_{v2}, \quad f_{v2} = 1 - \frac{\chi}{1 + \chi f_{v1}} \quad (23)$$

where d is the distance to the closest wall. The wall destruction function f_w is

$$f_w = g\left(\frac{1 + C_{w3}^6}{g^6 + C_{w3}^6}\right)^{\frac{1}{6}}, \quad g = r + C_{w2}(r^6 - r), \quad r = \frac{\tilde{\nu}}{\tilde{S}\kappa^2 d^2} \quad (24)$$

The model coefficients are

$$\begin{aligned} C_{b1} &= 0.1355 & \sigma &= 2/3 & C_{b2} &= 0.622, & \kappa &= 0.41 \\ C_{w1} &= C_{b1}/\kappa^2 + (1 + C_{b2})/\sigma, & C_{w2} &= 0.3, \\ C_{w3} &= 2.0, & C_{v1} &= 7.1 \end{aligned} \quad (25)$$

Coupled with Navier-Stokes equations, the Spalart-Allmaras turbulence model is solved using a finite-volume method, in which the convective flux is discretised using the first-order upwind scheme [Koomullil and Soni (1999)].

6 Methods of Variable Mass and Variable Stiffness for Flutter Calculation

Once the flight altitude and the flight Mach number are given, the happening of flutter can be judged by analyzing the generalized coordinate time response of each structural mode, which is solved from equation (4). The variation of flutter altitude with Mach number forms the flight flutter borderline.

In engineering, when the flutter does not happen at sea level at a given Mach number, the specified dynamic pressure of flutter must be obtained in order to confirm a practicable margin of flutter. At a given freestream Mach number, while the flutter calculations of a compressible flow are done in the time domain, the freestream dynamic pressure allows to be straightly increased to the critical flutter point. Due to the existence of mass dissimilarity, this dynamic pressure cannot be directly taken as the flutter one. That is to say, because of the fixed velocity (a given freestream Mach number), the fluid density inversely solved from the present dynamic pressure of flutter may be much larger than the atmospheric density in the flight condition, which violates the mass similarity rule.

At present work, methods of variable mass and variable stiffness are developed to calculate the dynamic pressure of flutter at the point of mass similarity. For the method of variable mass, the mass of an aircraft is increased to

a serial of multiples, denoted by $C_j(j = 1, 2, \dots)$, and the corresponding dynamic pressure of flutter denoted by Q_j are calculated, then the density, denoted by ρ_j , are solved from the definition of dynamic pressure. Let D_j represent the ratio of ρ_j to the atmospheric density at the given flight altitude. At a certain mass multiple, once C_j equals to D_j , the mass similarity rule is satisfied at an overweight state, and the dynamic pressure at that moment can be thought as the dynamic pressure of flutter. For the method of variable stiffness, the mass and the freestream dynamic pressure are kept invariable, a gradually minished stiffness, denoted by stiffness multiple N_j , will also lead to a flutter. The difference between this stiffness and the original one can be taken as the stiffness margin of flutter. Methods of variable mass and variable stiffness are correlative. It is easy to derive

$$N = 1/C \quad (26)$$

where N represents the stiffness multiple when the flutter happens using method of variable stiffness, C represents the mss multiple when the flutter happens at the mass similarity point using the method of variable mass.

Obviously, method of variable stiffness is much more timesaving than method of variable mass, despite the fact that the stiffness is no longer the original one. A synthetical consideration about the variation trend of the dynamic pressure of flutter varying with the mass and stiffness multiples will confirm a practicable transonic dynamic pressure of flutter.

7 Results and Discussion

Results have been obtained for two cases using the present transonic flutter computational method. In each case, the structural modal value of each grid node is obtained by a double linear interpolation method. In a physical time step, the calculation order is: firstly solving the time-accurate generalized aerodynamic forces by equation (8), secondly solving the generalized coordinates by equation (4), thirdly solving the longitudinal oscillation deformation of the wall surface points by equation (3) and generating the dynamic grids for the next physical time, and then repeating the above three steps at the next time loop. Finally, the generalized coordinate time response is obtained.

The first problem considered is about a double-wing, to which the flutter happens at sea level. Solutions with

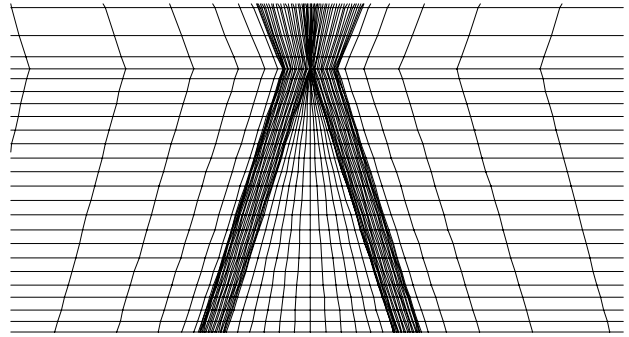


Figure 1 : Surface grid for a double-wing

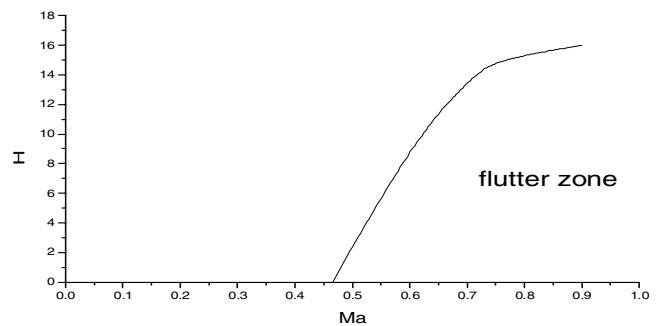


Figure 2 : Flutter borderline

Navier-Stokes equations are shown for computations performed on the H-H type multi-block grids, the Reynolds number based on the root chord length is 12×10^6 . Fig. 1 shows its surface grid. Fig. 2 shows the calculated flutter borderline. Fig. 3 and Fig. 4 respectively show the generalized coordinate time response for $Ma=0.45$ and $Ma=0.5$ at sea level, where $q(i)$ denotes the generalized coordinate time response of the i th-order structural mode. As a result, the calculated flutter velocity is 158m/s which is very close to the result 160m/s [Guo, Lu, and Cheng (2004)] calculated using the traditional doublet lattice method.

The next test case considered is about an aircraft model, to which the flutter doses not happen at sea level. The margin of flutter should be confirmed, so the methods of variable mass and variable stiffness are applied. Seven structural modes and natural frequencies are considered for the test cases: first bending mode of wing, first bending mode of fuselage, first bending mode of horizontal tail, first twisting mode of wing, second bending mode of fuselage, second bending mode of wing, second twist-

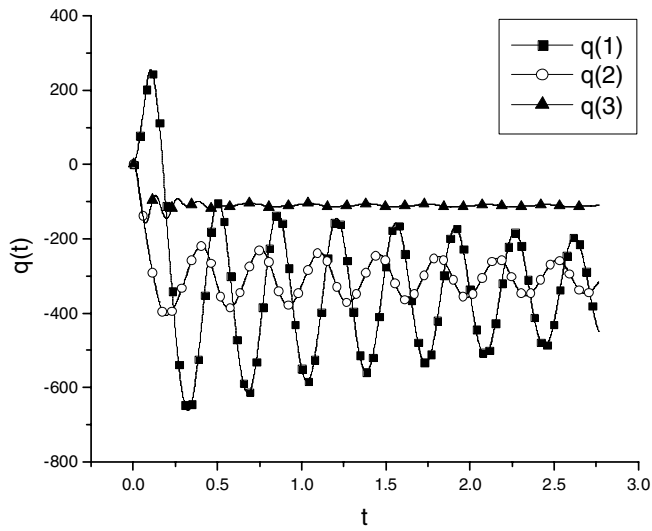


Figure 3 : Generalized coordinate time response (H=0km, Ma=0.45)

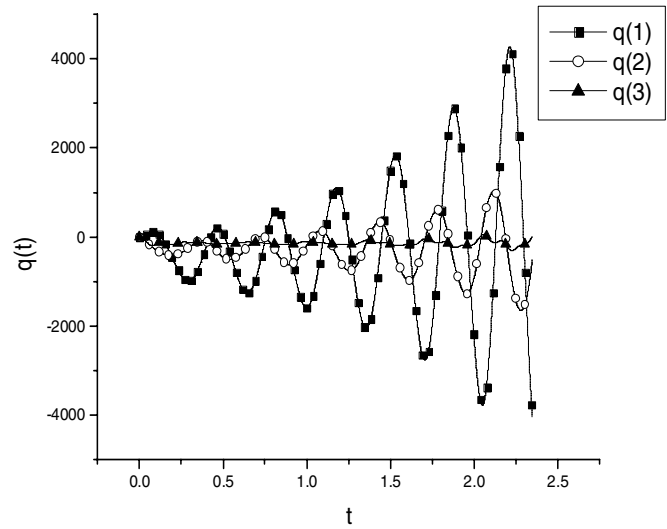


Figure 4 : Generalized coordinate time response (H=0km, Ma=0.5)

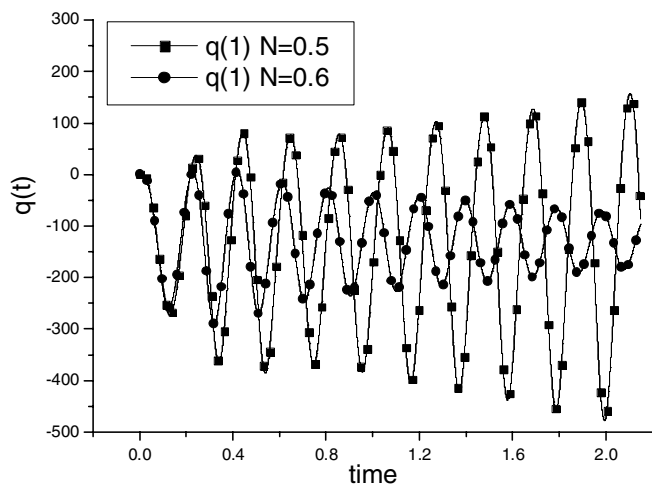


Figure 5 : Generalized coordinate time response with Euler equations

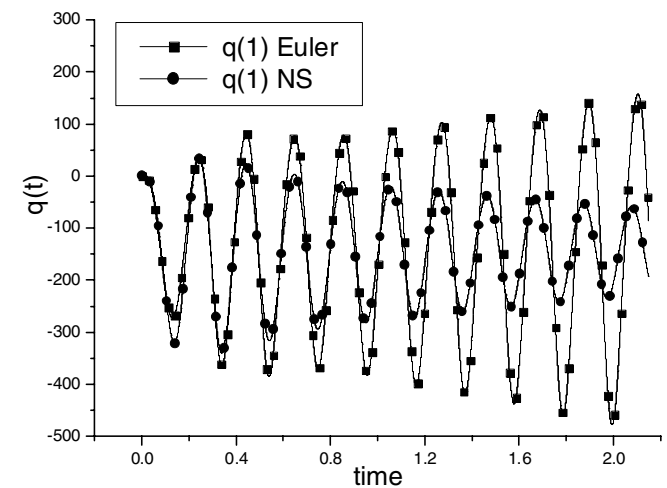


Figure 6 : Comparisons between Euler and Navier-Stokes equations at N=0.5

ing mode of wing. The H-H type multi-block grids are used. Cases at sea level are considered: the atmosphere density at sea level is chosen as the reference density, and the freestream Mach number is 0.9. For the calculation of the Navier-Stokes equations, the Reynolds number is 12×10^6 based on the root chord length. Some results are illustrated and analyzed as follows.

Fig.5 shows the generalized coordinate time response of the first structural modes when the stiffness is respectively reduced to 0.5 and 0.6 times of the original one with Euler equations, in which the abscissa is the time and the ordinate is the generalized coordinate. In Fig.5, the structure is convergent at $N=0.6$, but divergent at $N=0.5$, which means that the flutter has happened. The stiffness multiple at the critical state can be obtained by interpolation, while more intermediate values should be evaluated because of the severely non-linear properties in transonic range. Fig.6 is a comparison between Euler and Navier-Stokes equations at $N=0.6$. Theoretically, results from Navier-Stokes equations are more conservative than those from Euler equations, since the work that the aerodynamic forces do on the structure is less when Navier-Stokes equations are applied. Therefore, results shown in Fig.6 are reasonable.

8 Conclusions

Euler/Navier-Stokes equations coupled with structural equations of motion are applied to flutter computation in the time domain. Methods of variable mass and variable stiffness are developed to resolve problem of mass dissimilarity. As a result, a transonic flutter characteristic computational method, which is applicable to real problems in engineering, is established. Results of test cases prove the validity of the present method.

References

De, Guan (1994): *Aircraft Aeroelasticity Handbook*. Aviation Industry Press, China.

Gationde, Ann L (1995): A dual-time method for the solution of the 2D unsteady Navier-Stokes equations on structured moving meshes. *AIAA Paper* 95-1877.

Guo, Tongqing; Lu, Zhiliang and Cheng, Fang (2004): An Integrated Algorithm Method For Static Elasticity and Flutter. *Journal of Vibration Engineering*, Vol.17 No.4, China, Dec. 2004.

Jameson A.J. (1991): Time Dependent Calculations Using Multigrid, with Application to Unsteady Flows past Airfoils and Wings. *AIAA Paper* 91-1596.

Jameson, A.J; Schmidt, W. and Turkel, E. (1981): Numerical Solutions of the Euler Equations By Time-Stepping Schemes. *AIAA Paper* 81-1259.

Jameson, A.; Schmidt, W. and Whitfield, D. (1981): Finite Volume Solution for the Euler Equation for Transonic Flow over Airfoils and Wings including Viscous Effects. *AIAA Paper* 81-1265.

Koomullil, R. P. and Soni, B. K. (1999): Flow Simulation Using Generalized Static and Dynamics Grids. *AIAA Journal*, Vol 37, No. 12, Dec. 1999, pp 1551-1557.

Lu, zhiliang (2001): Generation of Dynamic Grids and Computation of Unsteady Transonic Flows around Assemblies. *Chinese Journal of Aeronautics*, 2001,22(1): 1-5.

Martinelli, L. and Jameson, A. (1990): Multigrid Solution of the Navier-Stokes Equations on triangular Meshes. *AIAA Journal*, 28, 1990, pp1415-1425.

P'ascoa, J. C.; Mendes, A. C.; Gato, L. M. C.; Elder, R. (2004): Aerodynamic Design of Turbomachinery Cascades Using an Enhanced Time-Marching Finite Volume Method. *CMES: Computer Modeling in Engineering & Sciences*, Vol. 6, No. 6, pp. 537-546

Shu, C.; Ding, H.; Yeo, K.S. (2004): Computation of Incompressible Navier-Stokes Equations by Local RBF-based Differential Quadrature Method. *CMES: Computer Modeling in Engineering & Sciences*, Vol. 7, No. 2, pp. 195-206.

Spalart, P.R. and Allmaras, S.R. (1992): A One-Equation Turbulence Model for Aerodynamic Flows. *AIAA Paper* 92-0439.

Thomas, P.D. and Lombard C.K. (1979): Geometric Conservation Law and its Application to Flow Computations on Moving Grids. *AIAA Journal*, Vol 17 No. 10, pp1030-1037.

Wang, B.; Zhang, H.Q., Chan, C.K.; and Wang, X.L. (2004): Velocity Fluctuations in a Particle-Laden Turbulent Flow over a Backward-Facing Step. *CMC: Computers, Materials, and Continua*, Vol. 1, No. 3, pp. 275-288.

